

# Measurement of $\varepsilon'/\varepsilon$ from the NA48 experiment

J. Ocariz\*

CERN, EP Division, CH-1211 Genève 23

E-mail: jose.ocariz@cern.ch

ABSTRACT: Using data collected in 1998 by the NA48 experiment, a preliminary measurement of the direct CP violation parameter  $Re(\varepsilon'/\varepsilon)$  is here presented, together with a discussion of the experimental method, data analysis and systematic studies. The result is  $Re(\varepsilon'/\varepsilon) = (12.2 \pm 4.9) \times 10^{-4}$ , and combined with the previously published NA48 result (based from data collected in 1997) gives  $Re(\varepsilon'/\varepsilon) = (14.0 \pm 4.3) \times 10^{-4}$ .

## 1. Motivation

CP violation was first established in the neutral kaon system. This phenomenon occurs due to an asymmetric mixing of  $K^0$  and  $\bar{K}^0$  in the physical kaon eigenstates, which leads to a non-zero amplitude for the decay of long-lived neutral kaons into two pions. This *CP violation in the mixing* is described by the mixing parameter  $\varepsilon$ .

CP violation can also occur through the interference of decay amplitudes to a given final state. In the neutral kaon system, this translates into a non-zero value for the *direct CP violation* parameter  $\varepsilon'$ , suitably defined in terms of the double ratio  $R$  of decay rates for charged and neutral two-pion final states:

$$R = \frac{\Gamma(K_L \rightarrow 2\pi^0)}{\Gamma(K_S \rightarrow 2\pi^0)} / \frac{\Gamma(K_S \rightarrow \pi^+\pi^-)}{\Gamma(K_L \rightarrow \pi^+\pi^-)},$$

$$= 1 - 6 \times Re(\varepsilon'/\varepsilon).$$

In the standard model framework, CP violation arises from the existence of three generations of quarks leading to an irreducible complex phase in the quark mixing matrix, and  $\varepsilon'$  is naturally non-zero. Calculations typically lie in a range  $0 \lesssim Re(\varepsilon'/\varepsilon) \lesssim 20 \times 10^{-4}$  (see [1] for a recent review). Previous experimental measurements can be found in [2, 3, 4, 5].

A preliminary result from NA48, based on data collected during the 1998 data-taking pe-

riod, is here reported. The experimental method and analysis technique follow quite closely the previous NA48 result [5], where more details can be found.

## 2. The NA48 method

The NA48 experiment is designed to measure  $Re(\varepsilon'/\varepsilon)$  with a final accuracy of about  $2 \times 10^{-4}$ , by collecting a sufficient number of all four kaon decay modes into two pions, at the same time and in the same fiducial volume. In this way, most systematics cancel in the double ratio, which reduces to

$$R = \frac{N(K_L \rightarrow 2\pi^0)}{N(K_S \rightarrow 2\pi^0)} / \frac{N(K_S \rightarrow \pi^+\pi^-)}{N(K_L \rightarrow \pi^+\pi^-)}.$$

NA48 uses two simultaneous  $K_L$  and  $K_S$  beams, both illuminating the detector in a very similar way. Having different decay lengths, only events occurring in the  $K_S$  decay region are used, and  $K_L$  events contribute to the double ratio with a weight given by their proper decay time, thus equalising both decay distributions. In this way, acceptance corrections cancel to a large extent.

High resolution detectors are used to select decays into two pions: a liquid krypton calorimeter for neutrals, and a magnetic spectrometer for the charged modes. A tagging station in the proton path to the  $K_S$  target allows identified decays to be tagged as  $K_S$ , in case of a time coincidence between detector and proton beam times, and  $K_L$  otherwise.

\*On behalf of the NA48 collaboration,  
<http://www.cern.ch/NA48/Welcome.html>

### 3. Beams and detectors

#### 3.1 The kaon beams

A primary 450 GeV proton beam from the SPS impinges a berillium target, produces a  $K_L$  beam, pointing to the fiducial decay region, and collimated along 126 m. A small fraction of the protons exiting the  $K_L$  target crosses the tagging station, where the time of passage of each single secondary proton is measured with a resolution better than 200 ps. Finally, these protons impinge a second target, producing a  $K_S$  beam 6 m upstream the fiducial region. This  $K_S$  beam traverses the AKS, a set of scintillators following a 3 mm thick iridium crystal. By rejecting  $K_S$  decays occurring upstream, this detector defines the beginning of the fiducial decay region, contained in a 90 m long vacuum tank, surrounded by scintillating anticounters. The  $K_L$  and  $K_S$  beams converge with a 0.6 mrad angle, and their axes cross at the liquid krypton calorimeter.

#### 3.2 Main detector

The spectrometer is made up of four drift chambers and a dipole magnet with a transverse momentum kick of 265 MeV/c. With a better than 100  $\mu$ m spacepoint resolution, transverse decay vertex positions are measured with a 2 mm resolution, thus allowing unambiguous  $K_L$  and  $K_S$  beam separation. Charged track momenta are measured with a resolution of

$$\frac{\sigma(p)}{p} = 0.5\% \oplus 0.009\% \times p,$$

( $p$  in GeV/c). Two plastic scintillator hodoscope planes measure charged event times with a resolution better than 200 ps.

A quasi-homogeneous liquid krypton calorimeter with a projective tower readout is used to detect neutral events, by measuring with great accuracy the energy, impact position and time of photons from  $2\pi^0$  decays. The detector is segmented into 13212 readout cells, with a  $2 \times 2$  cm<sup>2</sup> uniform cross-section. Current induced on electrodes is measured using pulse shapers with 80 ns FWHM and digitised with 40 MHz FADCs. Single photon energy is measured with a resolution

$$\frac{\sigma(E)}{E} = \frac{3.2\%}{\sqrt{E}} \oplus \frac{10\%}{E} \oplus 0.5\%,$$

( $E$  in GeV). Energy measurement is linear within 0.2% in a 5-100 GeV range. Spatial resolution is better than 1 mm above 25 GeV, and neutral time resolution is better than 250 ps.

Located downstream the electromagnetic calorimeter is an iron-scintillator sampling hadronic calorimeter, followed by a muon counter made up of scintillator planes sandwiched between iron walls.

#### 3.3 Triggers

The fully-pipelined, electromagnetic calorimeter readout, is used to trigger on  $\pi^0\pi^0$  events. Using horizontal and vertical energy deposition profiles, total energy and decay position are estimated. The efficiency is measured on neutral signal events to be  $(99.93 \pm 0.02)\%$ , with no difference for  $K_S$  and  $K_L$ .

The charged trigger operates at two levels. First level is based on coincidences between energy deposition in the calorimeters and charged hodoscope activity, and reduces the event rate with negligible inefficiency on signal events. The second level performs a fast, online event reconstruction to estimate  $\pi^+\pi^-$  decay vertex and invariant mass. It has about 5 % dead time and an efficiency of  $(97.75 \pm 0.05)\%$ . Charged trigger efficiency leads to a  $(-1 \pm 11) \times 10^{-4}$  correction to the double ratio  $R$ .

## 4. Data analysis

### 4.1 Event selection and background subtraction

#### 4.1.1 Charged modes

The dominant backgrounds for the  $K_{S,L} \rightarrow \pi^+\pi^-$  events come from the much more abundant semileptonic  $K_L$  decays, namely  $K_L \rightarrow \pi^\pm e^\mp \nu_e$  (“ $K_{e3}$ ”) and  $K_L \rightarrow \pi^\pm \mu^\mp \nu_\mu$  (“ $K_{\mu3}$ ”). They are rejected by excluding charged events in which there is a track consistent with being either an electron or a muon. Electron tracks are identified by a close to unity ratio  $E/p$  of electromagnetic cluster energy and track momentum, so that both tracks in candidate events are required to satisfy  $E/p < 0.8$ . Muon counter activity in time coincidence with event, and with hits near

an extrapolated track impact point, is used to identify muon tracks.

For good charged events, the  $\pi^+\pi^-$  invariant mass is measured with an average  $2.5 \text{ MeV}/c$  resolution, and  $m_{\pi\pi}$  for candidates is required to lie within a  $\pm 3\sigma$  energy-dependent window around the kaon mass. The  $\pi^+\pi^-$  transverse momentum is required to satisfy  $p_T^2 < 2 \times 10^{-4} (\text{GeV}/c)^2$ . In order to remove events with tracks near the beam hole, and get rid of  $\Lambda$  decays as well, a cut is made on the relative track momentum asymmetry.

The residual background in the charged  $K_L$  sample is estimated through a fit on a wide  $m_{\pi\pi}$  vs.  $p_T^2$  plane, and is  $(19 \pm 3) \times 10^{-4}$ . Figure 1 shows the result of this fit in the  $p_T^2$  distribution.

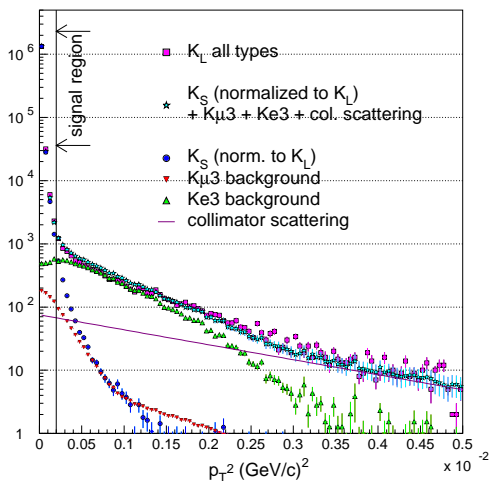


**Figure 1:**  $p_T^2$  distribution for  $\pi^+\pi^-$  candidates fulfilling the invariant mass cut.

#### 4.1.2 Neutral modes

Neutral candidates are selected from four-photon events, and background comes from  $K_L \rightarrow 3\pi^0$  events with two photons out of the calorimeter acceptance. The longitudinal decay vertex is reconstructed from the measured photon energies and positions, assuming their invariant mass is the kaon mass. A correctly reconstructed event must have two photon pairs with invariant masses  $m_1, m_2$  compatible with the nominal  $\pi^0$  mass. By computing a  $\chi^2$  variable, defined as

$$\chi^2 = \left( \frac{m_1 + m_2 - 2m_{\pi^0}}{2\sigma_+} \right)^2 + \left( \frac{m_1 - m_2}{2\sigma_-} \right)^2,$$

the optimal pairing is required to have  $\chi^2 < 13.5$ , and its distribution is shown on Figure 2. The residual  $K_L \rightarrow 3\pi^0$  background is estimated by extrapolating the event density in the  $\chi^2$  control window under the signal region, and is measured to be  $(6.6 \pm 2.0) \times 10^{-4}$ .

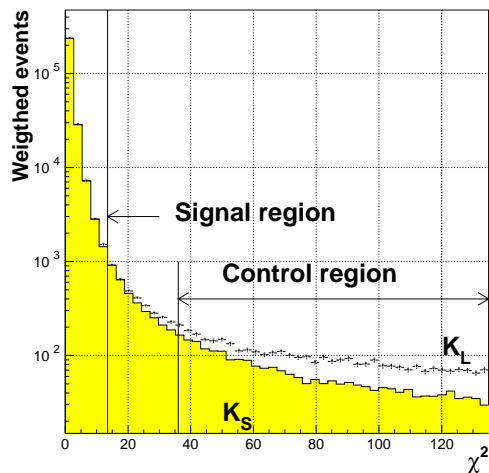


**Figure 2:**  $\chi^2$  distribution for weighted neutral  $K_L$  candidates, compared to the shape of a pure  $2\pi^0$  sample, obtained from neutral  $K_S$  events.

#### 4.1.3 Tagging

A signal event is tagged as  $K_S$  by comparing detector time and tagger activity, i.e. if there is a proton within a  $\pm 2 \text{ ns}$  around the event time. Otherwise, the event is tagged as  $K_L$ . Figure 3 illustrates the tagging technique.

Systematics related to the tagging technique can be measured directly for charged events, using beam separation from the reconstructed vertex. Tagging inefficiency, causing a  $K_S$  decay to be out of coincidence, is  $(1.97 \pm 0.05) \times 10^{-4}$  for charged events, while accidental tagging probability, due to unavoidable time coincidences between charged  $K_L$  events and proton activity in the tagger, is measured to be  $(11.05 \pm 0.01)\%$ .

Neutral tagging systematics are estimated by means of indirect methods. With neutral events containing photon conversions, any possible difference in tagging inefficiencies for charged and neutral modes is evaluated to be less than  $3 \times 10^{-4}$ ;  $3\pi^0$  events are used to estimate a possi-

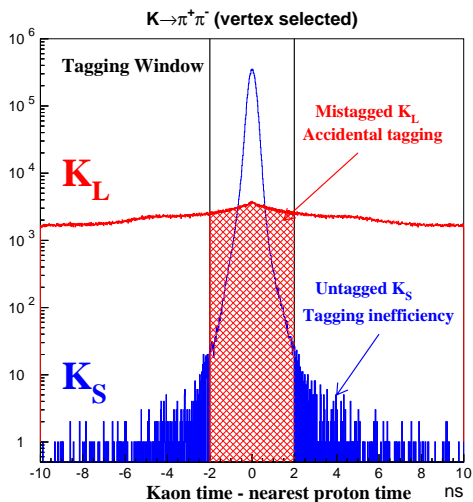


**Figure 3:** Minimum time difference between event time and proton time, for vertex-selected charged events.

ble difference in the accidental tagging, which is measured to be  $(0.3 \pm 4.2) \times 10^{-4}$ .

These systematics induce corrections on the double ratio  $R$ , estimated to be  $(0 \pm 3) \times 10^{-4}$  and  $(0.6 \pm 8.5) \times 10^{-4}$ , respectively.

#### 4.1.4 Energy and distance scale

The overall charged distance scale is defined by the spectrometer transverse dimensions, and a  $2 \times 10^{-4}$  systematic error on  $R$  is estimated from the drift chamber geometry tolerances.

The absolute neutral energy scale is obtained from the sharp rise in the longitudinal decay distribution of neutral  $K_S$  signal events, which is adjusted to coincide with the AKS position. A cross-check was performed by means of a  $\pi^-$  beam impinging a thin target, producing  $\pi^0$ 's and  $\eta$ 's with known decay position. The accuracy of the overall energy scale setting is estimated to be  $3 \times 10^{-4}$ .

Other sources of systematic uncertainty include the liquid krypton linearity (evaluated to induce a  $5 \times 10^{-4}$  uncertainty on the double ratio), uncertainties on the calorimeter transverse dimensions, calibration procedure, and non gaussian tails on the calorimeter response. Altogether, the total uncertainty coming from neutral event reconstruction is  $10.2 \times 10^{-4}$  on the double ratio  $R$ .

#### 4.1.5 Acceptance

$K_L$  and  $K_S$  acceptances are made very similar by weighting  $K_L$  events according to their proper decay time. Residual differences are studied by means of a detailed simulation of beams and detector response. A double ratio correction was calculated using a generated sample (about five times larger than event sample), estimated to be

$$(31.1 \pm 6.4 \pm 6.0) \times 10^{-4},$$

with systematic errors dominated by uncertainties in the beam positions and divergences.

#### 4.1.6 Accidental activity

Using two simultaneous beams, with correlated intensities, the double ratio  $R$  is to first order insensitive to event losses induced by beam-related activity. Possible effects are furthermore minimised by symmetric dead-time offline cuts. Residual effects are estimated by a software overlaying of “random” events (representing the typical beam activity) on top of signal event data. The resulting uncertainty on the double ratio is conservatively estimated to  $12.2 \times 10^{-4}$ .

## 5. Summary of corrections, systematics, and result

The previously published NA48 measurement was based on a sample collected in 1997, containing  $0.49 \times 10^6$   $K_L \rightarrow 2\pi^0$  events (the limitant mode for the statistical error). Several improvements were undertaken for the 1998 data taking period, and the accumulated sample corresponds to  $1.14 \times 10^6$   $K_L \rightarrow 2\pi^0$  decays, and correspondingly larger samples of the other three signal channels, namely 7.46, 4.87 and 1.80 millions for the charged  $K_S$ , neutral  $K_S$  and charged  $K_L$  modes, respectively.

The 1999 data taking was even more successful, and the collected signal sample includes about 2 millions of  $K_L \rightarrow 2\pi^0$  events. Analysis is currently in progress.

For all four signal modes, the fiducial 70 – 170 GeV range in kaon energy is divided into 20 bins. The double ratio and the various corrections (summarised in Table 1) are computed bin

Source	Correction ( $\times 10^4$ )	Error ( $\times 10^4$ )
$\pi^+\pi^-$ trigger efficiency	-1.4	11.5
Accidental tagging	+0.6	8.5
Tagging efficiency		3.0
Energy scale, linearity		10.2
Charged vertex	+2.0	2.0
Acceptance	+31.1	8.7
$2\pi^0$ background	-6.6	2.0
$\pi^+\pi^-$ background	+19.0	3.0
Beam scattering	-9.9	3.0
Accidental losses	+2.0	12.2
Total	+36.8	23.8

**Table 1:** Corrections and uncertainties to  $R$ 

by bin. The average value for the double ratio is

$$R = (0.9927 \pm 0.0017 \pm 0.0024),$$

where the first error is statistical and the second systematic. Part of the systematic error actually comes from the statistics of used control samples. This double ratio measurement translates into a result on the direct CP-violating parameter

$$Re(\varepsilon'/\varepsilon) = (12.2 \pm 2.9 \pm 4.0) \times 10^{-4}.$$

## 6. Prospects and conclusions

Combined with the previous NA48 publication, obtained from data taken in 1997, and taking into account the small correlation in systematic errors, the NA48 result is

$$Re(\varepsilon'/\varepsilon) = (14.0 \pm 4.3) \times 10^{-4}.$$

1998 data analysis continues, and some systematics are expected to be reduced, in particular those related to acceptance, tagging, energy scale, and accidental activity. The analysis of 1999 data is also in progress.

During the 1999 winter shutdown, an implosion of the beam pipe badly damaged all four drift chambers. 2000 beam period is being undertaken without spectrometer, and systematic studies related to neutral modes are addressed. The spectrometer repair has been granted, is currently in progress, and the full NA48 detector will be ready for data taking in 2001.

## References

- [1] M. Ciuchini and G. Martinelli, hep-ph/0006056.
- [2] G. Barr *et al.*, NA31 collaboration, *Phys. Lett.* B317, 233 (1993).
- [3] L.K. Gibbons *et al.*, E731 collaboration, *Phys. Rev. Lett.* 70, 1203 (1993).
- [4] A. Alavi-Harati *et al.*, KTeV collaboration, *Phys. Rev. Lett.* 83, 22 (1999).
- [5] V. Fanti *et al.*, NA48 collaboration, *Phys. Lett.* B465, 335 (1999).